Laboratory Evidence for Ion-Acoustic–Type Double Layers

Chung Chan, M. H. Cho, Noah Hershkowitz, and Tom Intrator
Nuclear Engineering Department, University of Wisconsin, Madison, Wisconsin 53706
(Received 9 January 1984)

The formation of an ion-acoustic–type double layer was observed in the laboratory for the first time. The rarefactive part of a long-wavelength ion-acoustic wave grew in amplitude because of the presence of drifting electrons. The corresponding current limitation led to the formation of the double layer.

PACS numbers: 52.35.Mw, 52.35.Dm

Double layers[1,2] are large potential steps that resemble sheaths but which do not occur at plasma boundaries. Potential steps as large as $2000T_e/e$, where T_e is the electron temperature and e the electron charge, have been seen in laboratory investigations.[3–9] These structures have monotonic potential profiles and have been identified as Bernstein-Greene-Kruskal solutions of the Vlasov-Poisson equations.[1] Another class of double layers, which are not monotonic but are preceded by negative potential dips, have been found in numerical simulations of electron-current–driven anomalous resistivity. Simulations by De Groot *et al.*[10] observed the formation of such double layers with $e\Delta\phi/T_e < 4$ in a short system (length $L \approx 141\lambda_D$, where λ_D is the Debye length) when the electron drift velocity v_d against an ion background satisfied $v_d \gtrsim v_e$, where v_e is the electron thermal velocity. Ion-acoustic double layers were later found by Sato and Okuda[11] in simulations with slower drift velocity ($v_d < v_e$) and a longer system ($L > 512\lambda_D$). The ion-acoustic double layers were small amplitude ($e\Delta\phi/T_e \lesssim 1$) and were found to evolve from a subsonic negative potential pulse propagating in the direction of the electron drift. Recent satellite data[12] suggest that auroral electron acceleration is associated with a series of small ion-acoustic double layers rather than a single large structure. Here we wish to report the first laboratory evidence for such ion-acoustic double layers. Our experimental results differ significantly from previous laboratory observations[4–9] in that previous experiments only studied the evolution of large-amplitude double layers with $e\Delta\phi/T_e \gg 1$.

We have found that ion-acoustic double layers evolve from long-wavelength ($\lambda \gtrsim 60\lambda_D$), low-frequency ($\lesssim 0.1f_{pi}$, where f_{pi} is the ion plasma frequency) ion-acoustic waves which were excited by pulsing a grid and thereby changing the electron drift across the target chamber of a triple-plasma device.[13] This device consisted of two source plasmas bounding a target plasma. Plasma potential and density in the three plasmas could be varied separately. The source plasmas were created by filament discharge in argon gas (operating pressure $p_0 \simeq 1\times10^{-4}$ Torr) with $T_e \simeq 2$ eV and electron-to-ion temperature ratio $T_e/T_i \simeq 10$. The primary electrons were trapped in the source chamber by multidipole surface magnetic fields.[14] Ions entered the target from the high-potential source through a low-transparency grid. The target plasma consisted mostly of cold ions produced by charge exchange on these drifting ions. The cold ions accumulated because they were electrostatically trapped (see Fig. 1) and had a much smaller loss rate than the drifting ions. The system was essentially one dimensional and the radial potential profiles were uniform within a 30-cm diameter. The target plasma density was $n \simeq 10^7$ cm^{-3} with the target chamber length $L \simeq 150\lambda_D$. Collision lengths involving charged particles and neutral particles were longer than the device so that wave propagation could be considered to be collisionless. The relevant parameters were electron plasma frequency $f_{pe} \simeq 30$ MHz, $f_{pi} \simeq 100$ kHz, and ion-acoustic velocity $c_s \approx 2.2\times10^5$ cm/sec.

The boundary conditions of the experiment were chosen so that no potential difference was applied between the two grids (b and c) which bounded the target plasma (see Fig. 1). However, there was a potential difference of approximately $2T_e/e$ between the high-potential and the low-potential source plasmas. Three grids c, d, and e were used to separate the target plasma from the low-potential source plasma so that the plasmas do not see grid d (the pulsing grid) as an effective anode. Time-resolved axial plasma potential profiles were obtained by recording the floating potential of a hot emissive probe with a boxcar "interferometer" averaging technique.[7] Plasma potential profiles were verified with data from Langmuir probes and gridded ion energy analyzers.

At time $t=0$, grid d was switched from 10 to about 4.5 V, or approximately T_e/e below the low-

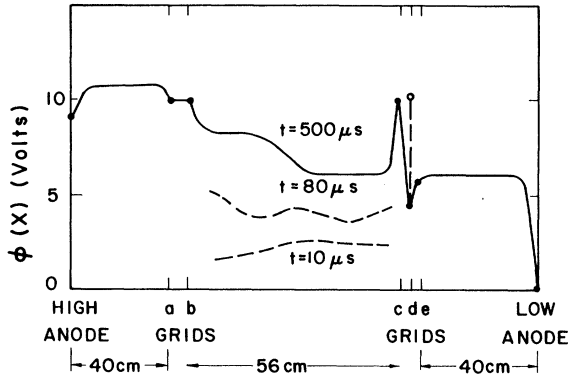

FIG. 1. Axial potential profile along the axis of the device. The open dot denotes the switching of grid d from 10 to 4.5 V at $t=0$ μs. Dashed lines denote profiles at different times.

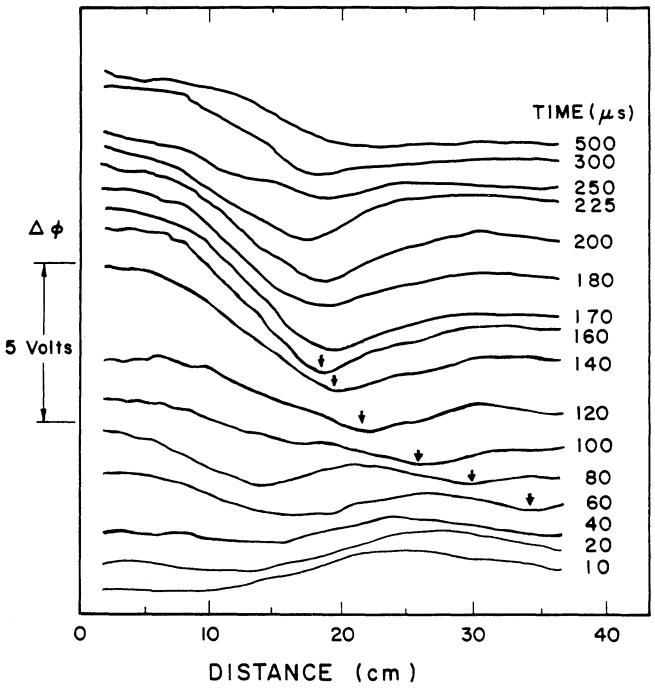

FIG. 2 Temporal evolution of the target plasma potential profile. Each profile is displaced for clarity. Arrows indicate the positions of the rarefactive pulse.

potential source plasma. At $t > 80$ μs, the target plasma potential became positive with respect to the potential on grid d and the Maxwellian tail of the low-potential source electrons which had overcome the potential of grid d was accelerated to $v_d < v_e$ by the potential difference between grid d and the target plasma potential near grid c. Note that the overall target plasma potential increased for $t > 0$. Data for plasma potential versus position in the target plasma are given in Fig. 2. A long-wavelength ($\lambda \approx 20$ cm) ion-acoustic wave was observed in the axial plasma potential profile 60 μs ($\approx 40\omega_{pi}^{-1}$) after switching grid d. The wave minimum, located at 34 cm, was observed to propagate from near the low-potential source in the direction of the electron drift. Similar temporal variations were also noted in the ion saturation current profiles. As the wave propagated, its amplitude increased while its velocity decreased from the original ion-acoustic velocity to almost zero at $t \approx 160$ μs (see Fig. 3). As the negative potential pulse grew deeper, an asymmetry in the potential between the upstream (right-hand) and the downstream (left-hand) sides also developed. At $t \approx 170$ μs, the double-layer maximum potential step on the left increased to $\Delta\phi \approx 2T_e/e$ while the potential step on the right only amounted to approximately T_e/e. This axial potential profile has a strong resemblance to the ion-acoustic–type double layers found in numerical simulations[11,15] as well as to analytical studies of the modified Korteweg–de Vries equation[16] and the Vlasov-Poisson equation.[17,18]

The potential dip began to fill in after $t \approx 250$ μs (a thermal-ion transit time across the double layer) and eventually became a steady-state monotonic double layer at $t \approx 500$ μs, roughly corresponding to a thermal-ion transit time across the system. This double layer had a small potential drop $\Delta\phi \lesssim T_e/e$ and appeared to be similar to the weak monotonic double-layer solution suggested by Kim.[19] The time history of the plasma potential revealed large-amplitude ($\delta\phi/\phi \approx 30\%$), low-frequency ($f \lesssim 10$ kHz $\approx 0.1 f_{pi}$) waves, shown in Fig.

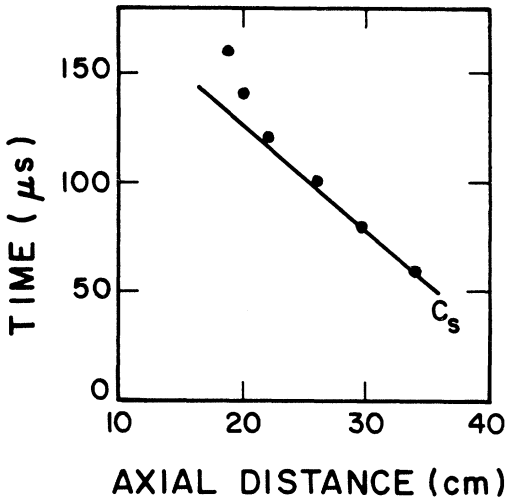

FIG. 3. The trajectory of the rarefactive pulse.

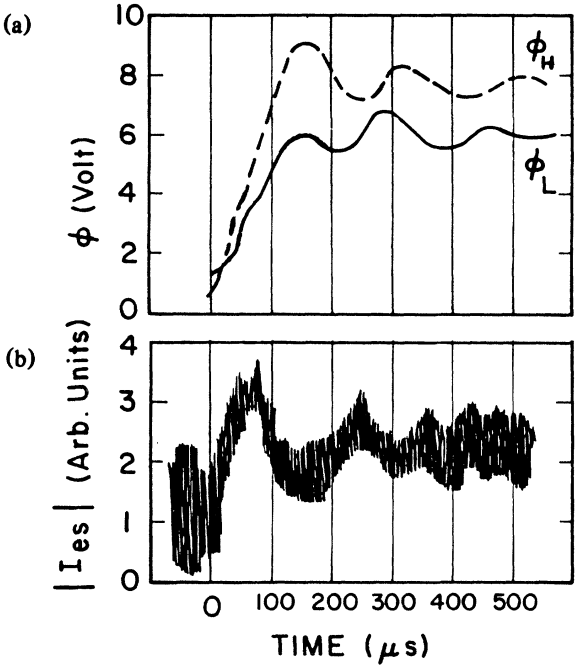

FIG. 4. Time history of (a) the target plasma potentials (ϕ_H, near high-potential source; ϕ_L, near low-potential source) and (b) the electron saturation current (I_{es}) collected by a single-sided Langmuir probe facing the low-potential source. The high-frequency oscillation may be induced by the probe (biased at +20 V) drawing electron current from the plasma.

4(a). The oscillation period was observed to increase with time consistent with an increase in the wavelength with time. The frequency satisfied $\omega = kc_s$ with k given by $2\pi/\lambda$ and λ estimated from the experiment. Thus the wave can be identified with the ion-acoustic regime. The time history of the electron current flow across the target chamber from the low-potential source gives evidence of current limitation [see Fig. 4(b)] when the negative potential pulse started to grow at $t \approx 80$ μs. The current reached a minimum at $t \approx 170$ μs when the potential dip reached its maximum amplitude (of the order of T_e/e). The observed current limitation came from the reflection of the left-going electrons (drifting electrons) by the negative potential dip. The current eventually settled at a constant value at $t \approx 500$ μs when the potential dip disappeared and a monotonic double layer formed.

Our experimental observations are very similar to the formation scenario[15-18] proposed for ion-acoustic–type double layers. The most significant feature observed in numerical simulations was the excitation of negative potential disturbances (ion-hole-like potential structures) which represent a transition from the current-driven ion-acoustic turbulence to a coherent nonlinear state. The rarefactive potential pulse propagated initially at the ion sound velocity in the direction of the electron drift. The negative pulse subsequently grew by exchange of energy with the drifting electrons[15-18] and the propagating velocity decreased to near zero. As the amplitude of the negative pulse became a significant fraction of T_e/e, the pulse blocked the electron current by reflecting the streaming electrons. The reflection of the drifitng electrons resulted in an ion-rich (positive space charged) region behind (downstream of) the negative potential pulse so that the potential profile became asymmetric. In our experiment an ion wave is excited by pulsing grid d which changes the right-side boundary conditions and produces an electron drift $v_d < v_e$. Landau growth and/or reflection dissipation[20] allows the rarefactive part of the wave to reflect the drifting electrons resulting in the formation of the ion-acoustic double layer.

Several important comparisons between the simulations and our experiments can also be made. First, the double layer observed in our experiment has a maximum potential step $\Delta\phi \approx 2T_e/e$ or a net potential drop of $1.4T_e/e$ which corresponds to the maximum values found in both simulations[11,16] and analytical studies of the Vlasov-Poisson equation.[17] Second, the widths of double layers found in simulations were also the same order of magnitude ($\approx 60\lambda_D$) as in our present experiment. Although early simulation results indicated that a system length much longer than our device was necessary for the formation of these double layers, Okuda and Ashour-Abdalla[21] later found that the system length can be as short as $128\lambda_D$ for $T_e/T_i \approx 20$ when a continuous plasma source is present. The dominant oscillating frequency was found to be $f < 0.1f_{pi}$ in both the simulations[11] and our experiments. In the simulation the oscillation frequency cascaded down from the original linearly unstable instability. As the amplitude of the negative pulse increased, current limitation which then led to the development of the asymmetric potential profile was seen in our experiment and the simulations.

The filling in of the potential dip and the formation of a steady-state monotonic double layer observed in the experiment differs from the simulation. In our experiment the dip could be filled in by ion-ion streaming instabilities. In the simulation the ion-acoustic double layers were observed to be unstable to soliton emission[11] with lifetime approximately equal to the transit time of an ion-acoustic soliton across the width of the double layer. The

ion-acoustic double layers were observed to come and go randomly when a continuous plasma source was present. In our experiments the filling in of the dip resulted in a steady-state monotonic double layer which was a stable configuration supported by the boundary conditions.

In summary, we have presented experimental evidence for the formation of ion-acoustic double layers previously observed only in numerical simulations.

This work was supported by the National Science Foundation through Grant No. ECS 83-14488 and by the National Aeronautics and Space Administration through Grant No. NAGW-275.

[1]L. P. Block, Cosmic Electrodyn. **3**, 349 (1972); G. Knorr and C. K. Goertz, Astrophys. Space Sci. **31**, 209 (1974).

[2]F. S. Mozer *et al.*, Phys. Rev. Lett. **38**, 292 (1977).

[3]N. Sato *et al.*, Phys. Rev. Lett. **46**, 1330 (1981).

[4]B. H. Quon and A. Y. Wong, Phys. Rev. Lett. **37**, 1393 (1976); P. Leung *et al.*, Phys. Fluids **23**, 992 (1980).

[5]P. Coakley *et al.*, Phys. Rev. Lett. **40**, 230 (1978).

[6]R. L. Stenzel *et al.*, Phys. Rev. Lett. **45**, 498 (1980).

[7]S. Iizuka *et al.*, Phys. Rev. Lett. **48**, 145 (1982).

[8]S. Iizuka *et al.*, Phys. Rev. Lett. **43**, 1404 (1979).

[9]Ch. Hollenstein, in *Proceedings of the Symposium on Plasma Double Layers, Roskilde, Denmark, 1982,* edited by P. Michelsen and J. Juul Rasmussen (Risø National Laboratory, Roskilde, Denmark, 1982), p. 187.

[10]J. S. DeGroot *et al.*, Phys. Rev. Lett. **38** 1283 (1977).

[11]T. Sato and H. Okuda, Phys. Rev. Lett. **44**, 740 (1980), and J. Geophys. Res. **86**, 3357 (1981).

[12]M. Temerin *et al.*, Phys. Rev. Lett. **48**, 1175 (1982).

[13]C. Chan *et al.*, Phys. Fluids. **26**, 1587 (1983).

[14]N. Hershkowitz *et al.*, Rev. Sci. Instrum. **51**, 64 (1980).

[15]M. K. Hudson *et al.*, J. Geophys. Res. **88**, 916 (1983); J. M. Kindel *et al.*, in *Physics of Auroral Arc Formation,* edited by S. I. Akasofu and J. R. Kan, Monograph Series, Vol. 25 (American Geophysical Union, Washington, D. C., 1981), p. 296.

[16]G. Chanteur *et al.*, Phys. Fluids **26**, 1584 (1983); K. Nishihara *et al.*, in *Proceedings of the Symposium on Plasma Double Layers, Roskilde, Denmark, 1982,* edited by P. Michelsen and J. Juul Rasmussen (Risø National Laboratory, Roskilde, Denmark, 1982), p. 41.

[17]A. Hasegawa and T. Sato, Phys. Fluids **25**, 632 (1982).

[18]H. Schamel, Phys. Scr. **T2**, No. 1, 228 (1982).

[19]K. Y. Kim, Phys. Lett. **97A**, 45 (1983).

[20]W. Lotko, Phys. Fluids **26**, 2176 (1983).

[21]H. Okuda and M. Ashour-Abdalla, Phys. Fluids, **25**, 1564 (1982).